Microbe-mineral interactions within kimberlitic fine residue deposits: impacts on mineral carbonation

Thomas Ray Jones[1,2]*, Jordan Poitras[1], Alan Levett[1],
Guilherme da Silva[1], Samadhi Gunathunga[1], Benjamin Ryan[3],
Andrew Vietti[4], Andrew Langendam[5] and Gordon Southam[1]

[1]School of Earth and Environmental Sciences, The University of Queensland, St. Lucia, QLD, Australia,
[2]CSIRO Agriculture and Food, St Lucia, QLD, Australia, [3]Cartledge Mining and Geotechnics, Brisbane,
QLD, Australia, [4]Vietti Slurrytec, Johannesburg, South Africa, [5]The Australian Synchrotron (ANSTO),
Clayton, VIC, Australia

The observation of photosynthetic biofilms growing on the Fine Residue Deposit (FRD) kimberlite produced by the Venetia Diamond Mine, Limpopo, South Africa suggests that processed kimberlite supports bacterial growth. The presence of this biofilm may aid in the acceleration of weathering of this ultra-mafic host material – a process that can sequester CO_2 via carbon mineralization. Laboratory and field trial experiments were undertaken to understand the microbe–mineral interactions occurring in these systems, and how these interactions impact geochemical cycling and carbonate precipitation. At laboratory scale it was discovered that using kimberlite as a growth supplement increased biomass production (up to 25-fold) and promoted microbiome diversity, while the inoculation of FRD systems aided in the aggregation, settling, and dewatering of kimberlitic slurries. Field trial studies combining photosynthetic biofilms (cultured in 3 × 1,000 L bioreactors) with FRD material were initiated to better understand microbially enhanced mineral carbonation across different depths, and under field environmental conditions. Over the 15-month experiment the microbial populations shifted with the kimberlitic environmental pressure, with the control and inoculated systems converging. The natural endogenous biosphere (control) and the inoculum accelerated carbonate precipitation across the entire 40 cm bioreactor depth, producing average 15-month carbonation rates of 0.57 wt.% and 1.17 wt.%, respectively. This corresponds to an annual CO_2e mine offset of ~4.48% and ~9.2%, respectively. Millimetre-centimetre scale secondary carbonate that formed in the inoculated bioreactors was determined to be biogenic in nature (i.e., possessing microbial fossils) and took the form of radiating colloform precipitates with the addition of new, mineralized colonies. Surficial conditions resulted in the largest production of secondary carbonate, consistent with a ca. 12% mine site CO_2e annual offset after a 15-month incubation period.

1 Introduction

The anthropogenic input of greenhouse gases into Earth's atmosphere is having a direct impact on its climate, resulting in the steady increase in surface temperatures around the globe (Masson-Delmotte et al., 2021). In response to this possible climate crisis, the onus is mounting on companies to lower their carbon footprints. By tailoring natural methods for carbon sequestration, that may be best accommodated using site specific processes already taking place, it may be possible to implement cost-effective carbon off-setting. Mineral carbonation is one such method that may lend itself to the *ex-situ* carbon sequestration that may be possible at mine sites.

Most of the carbon on Earth is housed in stable minerals that are derived directly or indirectly from the chemical weathering of silicate minerals. Known as mineral carbonation, this form of carbon sink has the capacity to store 106 Gt of carbon world-wide for an indefinite length of time (Lackner, 2003). Mineral carbonation occurs naturally over geological time, and at an accelerated rate within kimberlite lithology due to its ultramafic mineralogy which is highly susceptible to natural weathering at Earth's surficial conditions. This trait has been used historically to aid in the mining of diamonds and makes this material an attractive candidate for mineral carbonation. The Venetia mine, in Limpopo, South Africa, is an excellent natural laboratory and case study for possible on-site carbonation, as the ultramafic mineralogy and extensive on-site processing (crushing) capabilities of diamond mines are important criteria for carbon sequestration, i.e., increased surface area:volume ratio (Mervine et al., 2018). The kimberlite currently mined at Venetia is being recovered from a depth that has prevented this surface-based weathering to occur, allowing the opportunity for this reaction to be harnessed and guided - promoting the precipitation of secondary carbonates on a large, industrial scale.

Microorganisms can contribute to geochemical cycles in both surface and sub-surface environments, whether natural or industrial, via the dissolution and precipitation of minerals. These alteration mechanisms are starting to be utilized in the mining and environmental remediation industries, taking the form of biotechnology by utilising complementary biogeochemical cycles (Brandl et al., 2006; Dupraz et al., 2009; Gadd, 2010; Power et al., 2011; McCutcheon et al., 2017; Jones et al., 2023a). This process is facilitated primarily via the production of organic/inorganic acids, along with carbon dioxide, all reducing pH. Microorganisms utilize many different metabolic strategies to generate energy, though the primary mechanism for Earth surface mineral carbonation is photoautotrophy, where energy from sunlight is used to fix CO_2 from bicarbonate as a carbon source for biomass production. Through this process microbes act as a conduit for CO_2, drawing down the gas from the atmosphere and bringing it into contact with the intended carbonation host material.

Mineral carbonation is driven by the presence of available cations, an inorganic carbon source and a suitable, alkaline environmental pH, all of which are determined, or greatly influenced by, the mineral substrate in which it is intended to take place. Ultramafic substrates are often sought after for such uses, with kimberlites being the intended host for this project. Kimberlites are suitable due to their susceptibility to low-temperature alteration at near-surface conditions, generating the cations needed to bind with CO_3^{2-} available in an environment close to atmospheric CO_2 and sunlight. These conditions promote carbon sequestration via the formation of secondary carbonate minerals (see Wilson et al., 2009; Power et al., 2013; Sparks, 2013; Bodénan et al., 2014; Jones et al., 2023b). In addition to acting as a sequestration catalyst and conduit, microbes' effect other essential factors in this process. Weathering refers to the breakdown of the primary material, which supplies the cations (Ca, Mg, Fe) for carbonate precipitation. Microorganisms can promote geochemical changes by altering their immediate surrounding via the production of both organic acids (oxalic, malonic, lactic, and acetic acids, to name a few), and inorganic acids (Rodriguez and Fraga, 1999). This breakdown of primary minerals also impacts carbonation beyond the release of cations by also increasing the reactive surface area of the kimberlitic material. This creates not only potential carbonate nucleation sites, but also promotes microbial growth, which positively responds to the increased surface reactivity (Yoda et al., 2014; Xing et al., 2015). The development and use of kimberlitic material as a microbial co-substrate is an important factor to understand as it has implications for both carbon sequestration and the growth of the sequestration facilitating microbes.

The fine-grained kimberlite material being used as the primary carbonation host presents potential challenges to the carbonation process via the formation of clay rich impermeable layers. The deposition of clay can create a disconnect between the intended inorganic carbon source (atmosphere), and the intended host material (sub-surface kimberlite). On-site, this occurs during the settling of the material after processing, where the fine clays and clay-sized particles create an impermeable layer that separates the underlying kimberlite from the atmosphere.

This work was developed as part of Project CarbonVault™, an initiative undertaken by De Beers investigating the potential of using mineral carbonation to offset mine emissions. Understanding the microbial activity already occurring in the natural breakdown and transformation of mined kimberlite material at surficial conditions from blue ground → yellow ground, will aid in unlocking potential bioprocesses that can be upscaled and utilized by industry.

It is the aim of this study to assess the potential for biogeochemical mineral carbonation in fine grained, mined kimberlite, thereby transforming a waste material into a resource by off-setting emissions of a mine site.

Two modules are presented. Part A - representing a laboratory investigation, and Part B – a field trial. Lab scale experimentation was used to gain an understanding of the microbe-mineral interactions taking place between the Venetia FRD material, and endogenous, photosynthetic biofilms, also sourced from Venetia. Categories of investigation included: Does kimberlite act as a growth substrate and how does the environmental pressure of the FRD influence the microbiome?; What is the potential impact of the microbes on the aggregation of the FRD material?; How does the inoculation with microorganisms affect the layering of FRD during deposition.

The results of the laboratory module were then used in the experimental design of the field trial study – methods and results presented separately.

2 Materials and methods

2.1 The Venetia diamond mine – site characterization and sampling

The crushed kimberlite material used in this study was sourced from Venetia, South Africa's largest diamond producing mine, located in Limpopo, South Africa (22°25′59″ S, 29°18′50″E) (Figure 1A). The Venetia kimberlite group contains multiple facies and is made up of 12 occurrences: 11 pipes, and 1 intrusive dyke (Allsopp et al., 1995). The kimberlite currently being extracted and processed from Venetia are dominated by phyllosilicates, primarily serpentine minerals and smectites (19.0 wt.% and 36.6 wt.%, respectively), with diopside present at an average abundance of 20.5 wt.% (Mervine et al., 2018). Kimberlite residue from the Ventia mine includes Coarse Residue Deposit (CRD) materials (>0.8 mm) and Fine Residue Deposit (FRD) materials (< 0.8 mm).

For the laboratory experiments, dry Fine Residue Deposit (FRD) kimberlite was collected from the Venetia diamond mine, Limpopo, South Africa in 2017 (Figure 1 A & C) into plastic mesh bags, which allowed the kimberlite to dry during storage. This material represents the smallest size fraction of processed kimberlite produced via the on-site diamond extraction process, consisting of grains <800 μm and clays that weather out from the kimberlite matrix during processing.

For the field trial experiment, bulk kimberlite was collected directly from the Venetia mine Run of Mine (ROM; September 2019) and transported to the De Beers Group Technology SA research facility, where it was then crushed in potable water to achieve a grain size representative of the Venetia FRD material (≤ 800 μm), and used immediately in this field trial experiment.

2.2 The Venetia microbes

Biofilm (ca. mm thickness) used in the laboratory experiment, was sampled from two nearby (ca. 5 m apart) locations from within the FRD residue area at the Venetia mine site (Figure 1B) using sterile transfer pipettes and placed into 2 × 5 mL ICP tubes for transport to UQ for culturing and molecular biological analyses. The samples retained for molecular biological analyses were preserved in Lifeguard solution and stored at −20°C until the experiments were completed.
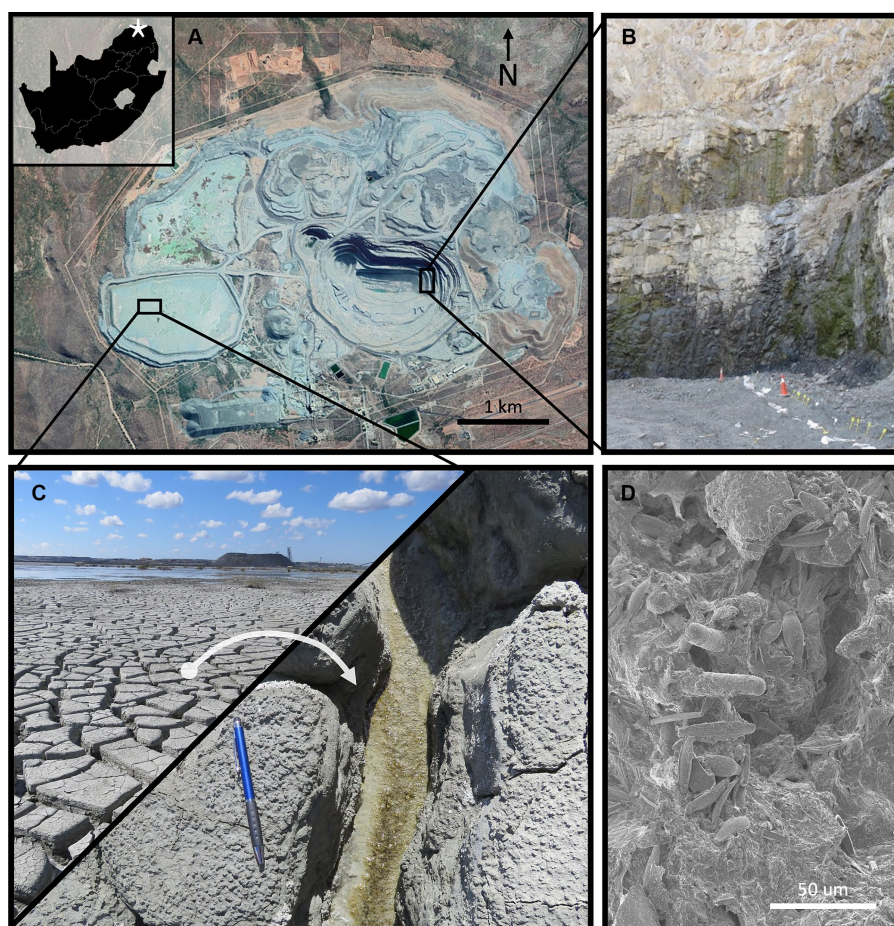
FIGURE 1
(A) A Google Earth satellite image of the Venetia diamond mine, Limpopo, South Africa, its location indicated by the star on the inset image (22°25′59″S, 29°18′50″E) of South Africa. **(B)** Benches 29 and 30 as viewed from the pit floor (K1 – East), showing water seepage through the kimberlite and the location of a well-established biofilm that was sampled for use in the field trial experiment. **(C)** Photographs of the Venetia diamond mine Fine Residue Deposit (FRD; < 800 μm grain size) with biofilm growing within the dehydration cracks; this biofilm was used for the lab scale experiments. **(D)** Secondary Electron SEM of the microbes sampled from the pit wall **(B)** revealing a diverse microbiome (bacteria, cyanobacteria, fungi, and diatoms) that has coated and intermixed with its kimberlite substrate.

The microbial biofilm used in the field trial was initially collected from within the Venetia pit (Figures 1A,C). Two, 20 L buckets were each filled with approximately 15 kg of cm-scale biofilm, associated water, and kimberlitic material attached to biofilm. The biofilm was sampled toward the base of the active pit, i.e., below the groundwater table, in area K1, on benches 29 and 30 (Figure 1B).

2.3 Laboratory biofilm growth and harvesting

One mL sub-samples of the two biofilms (collected from the FRD; Figure 1B) were pooled and inoculated into 2×5 L plastic tanks with 2 L of BG-11 media (Ripka et al., 1979) and incubated at room temperature (24°C) with window exposure to sunlight to support growth, approximately comparable to field conditions. One of the bioreactors was supplemented with 20 g of FRD, i.e., reflecting a 1% by mass growth substrate. Phenotypically, the FRD biofilm composite settled to the bottom of the culture vessel and developed a more intense green color suggesting enhanced cyanobacterial growth over the non-FRD, BG-11 culture system. The cultured microorganisms that were not given the FRD amendment were used for the accelerated growth (FRD co-substrate) experiment and for the microbe-mineral mixing – mineral carbonation experiment, while the biofilm cultured with the FRD amendment was selected for use as a source of biology for the accelerated settling experiment.

2.4 Kimberlite as a co-substrate

To examine the effect of FRD on the growth of biomass, i.e., serving as a co-substrate, 5 enhanced growth environments were set up (in duplicate) including the BG-11 growth control (from above). Using autoclaved 500 mL beakers, 360 mL of sterile BG-11 media were inoculated with 40 mL of BG-11 cultured biofilm. The inoculum was prepared by collecting 200 mL of 'biofilm' (microbial mats + media), rinsed two times with sterile saline water to remove spent media, before adding 360 mL of the BG-11 media for use in the co-substrate culture experiment. Before inoculum, the biofilm was homogenized using a magnetic stir plate for 1 h. Once homogenized, 40 mL of the inoculation was added to each (of 12) beaker(s). To create the co-substrate, a 10 wt% FRD slurry was made by combining dry FRD and dH$_2$O, using a magnetic stir plate to homogenize the suspension. Three 10 mL sub-samples of slurry were taken to determine dry weight. This slurry was added to the experimental beakers in increasing amounts of FRD; 0 g for the BG-11 controls, then 0.1, 0.95, 2.375 and 4.75 g/L FRD. Each

system was gently mixed using a sterile, glass stirring rod, then covered with serine wrap to minimise water evaporation and left in a sun lit area to incubate for 4 weeks. At the end of the growth period, the beakers were carefully decanted making sure not to lose any macroscopic materials. After gross decantation a sterile transfer pipette was used to remove any remaining liquid. A 250 μL aliquot of the aqueous biofilm was sampled from each system for DNA analysis (see below). All the systems were then washed with sterile saline water (200 mL) to remove spent media, again decanting the fluid, and dried at 40°C for 1 week. Once dried, the total mass of the material was weighed, with the original weight of BG-11 salts and the kimberlite co-substrate removed from the total weight to provide the total dry biomass produced. Note, the uptake of nutrients from the BG-11 culture media and co-substrate from the kimberlite could not be determined but are considered at the level of trace nutrients relative to biomass formation, as well as balancing each other out from a nutrient-biomass perspective.

2.5 Microbial driven de-watering; settling of fines

The settling properties of FRD mixed with biofilm was studied using 5 g/L FRD – BG-11 cultured photosynthetic biofilm as a dewatering agent. De-watering is possible via the adsorption of fines, i.e., mineral/clay particles from water, to biofilm, promoting settling by functioning as an agglomeration agent (Costa et al., 2018). The settling experiment was run using 100 mL graduated cylinders with 100 mL 10% w/v FRD slurry. Differing amounts of biology (wet wt. biofilm) was added to the systems (1, 5, 10, 15, and 20 cc) as well as controls, to which water was added to maintain identical volumes for Optical Density (OD) analysis.

The experiments were run with two different inoculation periods to assess how the ability of the microbes to settle the fines changed with increased time in contact with kimberlite. The first run had no kimberlite incubation time, where the settling measurements were taken immediately after inoculation. The second test had a kimberlite inoculation period of 14 days, after which the fines were re-suspended and settling rates measured. All systems were run in duplicate for 7 days and sampled at 1 h, 3 h, 6 h, 12 h, 24 h, 48 h, 96 h, and 168 h. To maintain comparative volumes across the different systems, all microbial additives were made up to the same volume (See Table 1). Once all the components for each system were combined (via inversion) a pipette was used to sample the systems at 1 cm and 10 cm depths. All OD measurements were made using a Synergy™ HT Multi-Detection Microplate Reader using a wavelength of 600 nm.

TABLE 1 FRD settling, experimental design.

	FRD Slurry	Biofilm	DI Water
Control systems	100 mL 10% FRD	0 cc biofilm	30 cc water
1 cc systems	100 mL 10% FRD	1 cc biofilm	29 cc water
5 cc systems	100 mL 10% FRD	5 cc biofilm	25 cc water
10 cc systems	100 mL 10% FRD	10 cc biofilm	20 cc water
15 cc systems	100 mL 10% FRD	15 cc biofilm	15 cc water
20 cc systems	100 mL 10% FRD	20 cc biofilm	10 cc water

2.6 Biofilm growth under FRD settling conditions

To ascertain the ability of the Venetia microbes to grow within the FRD and how burial with FRD may hinder growth, two systems were initiated into which FRD material was repeatedly deposited to mimic on-site FRD deposition. These systems were set-up in 70 mL Sarstedt Specimen Containers, both initially filled with 50 mL of DI water. A 2 g (wet weight) microbial inoculation was added to one system, while the control was kept sterile. After 1 week, and for the following 4 weeks (5 in total), 5 g of FRD material was deposited directly into the specimen containers. After the 5 deposition cyclings, each system was fitted with a loose-fitting lid and stored in a well-lit area for a further 6 months.

2.7 Field trial biofilm growth and harvesting

Microbial material collected from Venetia (See section 2.2) (Figure 1D) was transferred from the Venetia mine to the De Beers Group Technology SA facility in Johannesburg where it was homogenized by hand mixing and divided between three bioreactors that were each filled with 1,000 L of BG-11 medium (Ripka et al., 1979) (Figures 2A,B). An enriched medium was created based on the cumulative addition of 10 X strength BG-11 medium, divided over a four-month growth period.

To concentrate/de-water the microbial biomass generated in the bioreactors (Figure 2A), 20 kg of high surface area (<800 μm FRD) kimberlitic material was added to each bioreactor to accelerate settling of the biomass (promoted by adsorption and aggregation as describes in sections 2.5 and 2.6). This was important as large sections of microbial mats were floating on the surface and supported by gas bubbles due to oxygen production (a by-product of photosynthesis) (Figure 2B). After 24 h settling of the kimberlite-biomass composite ca. 90% of the spent culture medium was removed, leaving the microbial biomass FRD-kimberlite mix on the floor of each bioreactor tank.

2.8 Field trial FRD-bioreactor

'Homogenous' conditions: 625 kg of unweathered FRD material was split equally and mixed into the three de-watered bioreactors and mixed thoroughly using shovels. This material (FRD (625 kg) + FRD (aggregation) (3 × 20 kg) + wet weight biofilm + water = 902 kg) was then transferred into an IBC representing $T = 0$ for the weathering experiment (Figure 2C - foreground). To mimic the closed system conditions present at the Venetia FRD in the experimental IBC, the stop-cock at the bottom of the IBC was left closed.

2.9 Field trial control system

A control system was run alongside the inoculated FRD experiment. For this system, 685 kg of FRD (matching the total FRD used in the microbial treated system) of dry FRD was transferred into an IBC along with the continuous addition of city water to mimic the starting water saturation within the biotic experiment, which equalled 217 L (system totalling 902 kg) of water (Figure 2C - background). This control system was also left closed to represent on-site FRD conditions. After deposition and settling, the FRD levels within the inoculated and non-inoculated 1m³ IBCs were approx. 50 cm deep. Both IBCs were trimmed to ca. 60 cm height to allow exposure to sun and rain (weathering conditions) and access for sampling.

2.10 Field trial sampling

Samples of surface kimberlite from both the inoculated- and the control-system were sampled and transferred into sterile 50 cc Falcon tubes over the course of the experiment: $T = 0$ (January 2020); $T = 4$ months (May 2020); $T = 9$ months (October 2020); and $T = 15$ months (April 2021). Material sampling from the surface layer was done using a trowel cleaned with 70%$_{(vol./vol.)}$ ethanol.

At 15 months, a depth profile was collected from both systems using a 60 mm diameter aluminium pipe that was repeatedly hammered into the material in the IBC (measured for depth) and withdrawn, bringing material to the surface. The surface layer represents the top 10 cm of the system, and the three subsequent depths are composites of material in each underlying 10 cm layer. To minimise and edge effect, all samples were collected toward the middle of the IBC, avoiding previous (flagged) sample sites.

2.11 Material embedding and lapidary for BSE-SEM, MLA, and XFM analyses

Petrographic sections of microbe-mineral composites were prepared material sampled from both the laboratory study and field trial experiments. To capture the growth of biofilm in these clay rich materials (FRD) in *in-situ* conditions, the samples were subjected to a multi-step embedding protocol, developed to preserve biofilm while maintaining the *in-situ* structures of the FRD material. This protocol was developed with the laboratory samples and used again on the field trial samples. Materials collected from the experiment and transported in 50 cc Falcon tubes were oven dried at 40°C for 24 h before being dehydrated using 3 × 100% ethanol treatments. The embedding procedure was done in the transport tube to maintain any natural, *in-situ* intergranular cements and structures preserved during sampling. Each sample was then embedded sequentially, with two resins. LR White, a hydrophilic resin was used initially as it was unlikely that these clay-rich materials were completely devoid of water; 10 mL of this resin was allowed to flow through the samples by gravity, three times prior to setting anaerobically at 60°C for 48 h. Once hardened, Epo-Tek 301 resin was vacuum infiltrated to further ensure the rigidity and strength required for sample polishing. Each of the samples were then cut and formed into sections ~150 μm thick to ensure the stability of the biogenic carbonate/cements.

2.12 Scanning electron microscopy (SEM)

Material prepared for secondary electron Scanning Electron Microscopy (SEM) analysis was fixed with 2.5%$_{(aq)}$ glutaraldehyde and
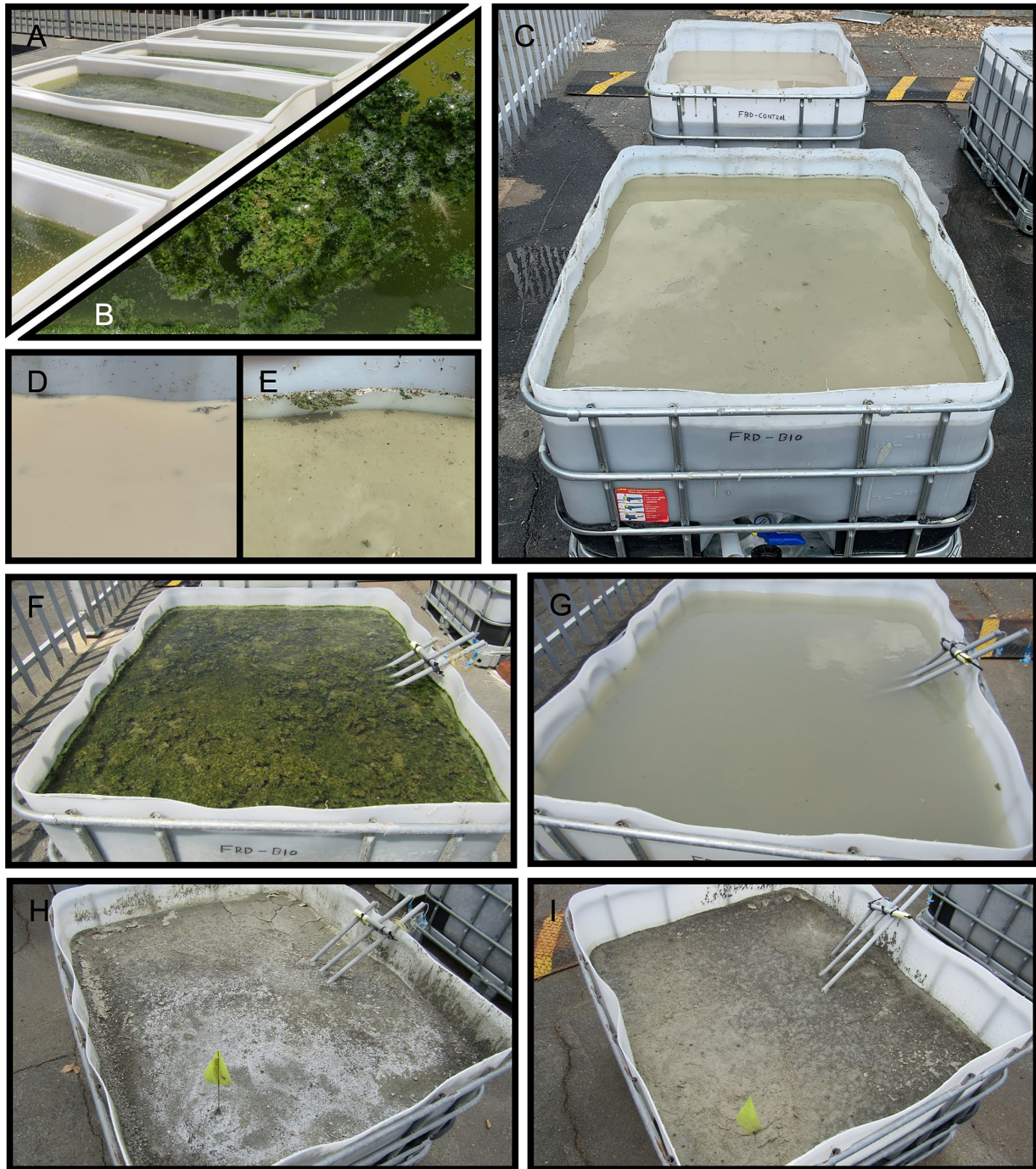
FIGURE 2
(A) The bioreactors shown just prior to inoculation into the FRD experiment. **(B)** A floating portion of the Venetia biofilm after ~4 months of growth within the bioreactors. **(C)** The FRD field trial experiments (bio-treatment = foreground, control = background) at *T* = 0. Tiles **(D)** (control) and **(E)** (bio-treatment) show the surface of the systems after 6 h. The control system showing no settling of fines within the overlaying water, whilst the bio-treatment shows clear water, indicating a significant degree of settling catalyzed by microbial presence. The inoculated **(F)** and control **(G)** systems after 4 months, coinciding with the end of the wet season in Johannesburg (Oct – April). The inoculated **(H)** and control **(I)** systems toward the end of the field trial study (~15 months). The microbial system shows the presence of white evaporites on its surface.

stored at @ 4°C for 24 h. All samples were then dehydrated using an ethanol dehydration series (20, 40, 60, 80%, 3 × 100%), and dried using a hexamethyldisilizane series with 100% ethanol (1,3, 2,2, 3,1, 3,0). Prior to microscopy, samples were placed in a vacuum oven overnight @ 40°C, plasma cleaned (Evactron Plasma Cleaner) and carbon coated (Quorum Q150T carbon coater). Field Emission Scanning Electron Microscopy (FE-SEM) was undertaken on a JEOLJSM – 7100F at an accelerating voltage of 20 keV for back scattered and between 2 and 4 keV for secondary electron imaging with a working distance of 5–10 mm.

2.13 Synchrotron X-ray fluorescent microscopy (XFM) and mineral liberation analysis (MLA)

Applicable for both laboratory and field trial work - elemental mapping of the 150 μm thick slides were mapped using the XFM Beamline at the Australian Synchrotron, Clayton, Australia (Paterson et al., 2011; Howard et al., 2020). A monochromatic 12.9 KeV X-ray beam was focused to 2 μm using a Kirkpatrick-Baez mirror pair. Overview scans were run with 20 μm pixels, which were decreased to 2 μm for high resolution maps captured by a 384 element Maia detector (Siddons et al., 2014). Image data was analyzed with GeoPIXE (Ryan et al., 2014) to produce elemental of the experimental systems. Mineral Liberation Analysis (MLA) was performed on the same samples used for XFM analysis, using a FEI Quanta 600 Mk2 MLA system; all MLA processing was done via the software MLA Dataview v.3.

2.14 Chemical analyses

To understand the geochemical changes in the field trial studies, major oxides were measured within the surface material (0–10 cm), collected at each time point (T = 0, 4, 9 and 15 months), and from each depth sample collected at 15 months (as above) (Figures 2, 3). Ten g sub-samples were collected from each sample, oven dried at 45°C for 1 week, then crushed using an agate mill to ca. 100 μm grain size. ICP-OES of the digested samples was undertaken using a Perkin Elmer Optima 8300DV Inductively Coupled Optical Emission Spectrometer (ICP-OES). Total Organic Carbon (TOC; ALS Laboratories; C-IR06a - HCl (25%) leach at high temperature for 1 h to expel carbonates as CO_2, residue analyzed for C by induction furnace/IR.) analyses were performed to estimate the bacterial inoculum.

2.15 DNA sampling, extraction, sequencing, and analysis

Laboratory phase – DNA samples were taken from each experimental system of the accelerated growth experiment to determine how the microbial population changed under the environmental pressure caused by the addition of the FRD material. These samples were submerged in 250 μL LifeGuard® Soil Preservation Solution (Qiagen) before DNA extraction, amplification of 16S rRNA genes and sequencing at the Australian Centre for Ecogenomics. Cell lysis was achieved by bead beating, followed by DNA extraction using DNeasy PowerSoil Pro Kit (#47016, Qiagen, Germany). Amplification of the V6-V8 portion of the 16S rDNA gene, using the universal primer set 926f (5′-TCGTCGGCAGCGTCAGATGTGTATAAGA GACAGAAACTYAAAKGAATTGRCGG-3′) and 1392wR (5′-GTC TCGTGGGCTCGGA GATGTGTATAAGAGACAGACGGGCGG TGWGTRC-3′) with modifications to contain the Illumina specific adapter sequence. Library preparation was done using workflow methods outlined by Illumina (#15044223) with the exception that the NEBNext® Ultra™ II Q5 Mastermix (New England Biolabs #M0544)

was used in standard PCR conditions. Agencourt AMPure XP beads were used to achieve DNA purification (Beckman Coulter, Brea, CA, United States)., which was then indexed using Illumina Nextera XT 834 sample Index Kit A-D (Illumina FC-131-1002, San Diego, CA, United States) in the mastermix to assign unique 8-bp barcodes. A MiSeq instrument with paired-end sequencing was used to pool Equimolar concentrations of the indexed amplicons (Illumina, San Diego, CA, United States) with a 600-cycle V3 300-bp reads. Total read counts ranged from 25,912 to 102,331, with an average of 70,525.

Demultiplexed sequences were processed using methods consistent with Coleman et al. (2021). Cutadapt (v. 3.5) was used to remove the universal primer sequences (Martin, 2011 – EMBnet journal). Reads were subsequently duplicated and filtered using QIIME2 (v. 2022.2), with chimeras removed by DADA2 (−-p-2 trunc-len-f 250 and --p-trunc-len-r 230) (Callahan et al., 2017). The resulting amplicon sequence variants (ASVs) were taxonomically assigned using the nonredundant SILVA database (v. 138, clustered at 99% identity) (Quast et al., 2013). Amplicon data filtration and analyses were performed in R (v. 4.1.3). The following ASVs were discarded: sequences not classified below the phylum level, sequences classified as chloroplasts or mitochondria, sequences not determined to be either archaeal, bacterial or fungal in origin, and ASVs with an abundance of <0.1%. Heatmaps were produced using ggplot2.

Field trial phase – sterile 15 cc Falcon tubes were filled with material from each sampling point / location and submerged in LifeGuard® Soil Preservation Solution (Qiagen) prior to transport from Johannesburg to Australia. Using a laminar flow cabinet, 0.5 g subsamples were taken from each system using a sterile spatula and sent for DNA extraction, amplification of 16S rRNA genes and sequencing using the Illumina Miseq platform at the Australian Centre for Ecogenomics as mentioned above.

Raw sequences were analyzed using MOTHUR platform (v1.48.0) following the pipeline provided in (Gagen et al., 2018). The resulting operational taxonomic Unit (OTU) table was subsampled to the smallest sequence library size (n = 3,283) and equalized to obtain the same sequencing depth before analysing to determine the species richness, Shannon equitability, Invsimpson diversity and Jaccard dissimilarity calculations using R (Xia et al., 2018). Heat maps were generated using the same OTUs to demonstrate the mean relative abundance of major microbial lineages across samples. The microbial lineages that showed a mean relative abundance of <0.5% (at family level) or < 1% (at phylum level) were aggregated and presented as "Other" in the heat maps.

Data pre-processing and formatting were conducted in the R platform (v. 4.2.3) using the tidyverse package (Wickham et al., 2019). The Operational Taxonomic Units (OTUs) tables, generated through MOTHUR analysis, served as the basis for computing Jaccard distances. This task was accomplished using the 'vegdist' function from the vegan package (Oksanen et al., 2019). The resulting distance matrices were employed in constructing Non-Metric Multidimensional Scaling (NMDS) ordination plots. These plots facilitated the exploration of dissimilarities in microbial community composition between inoculated FRD and FRD controls across various sampling times and depths. The stress values obtained from the NMDS analysis were utilized as a metric to assess the goodness of fit. Data visualization was carried out in R using the ggplot2 package to enhance the clarity and interpretability of the findings.

3 Results: Part A – laboratory based studies

3.1 Kimberlite as a co-substrate

The addition of kimberlite to BG-11 media enhanced the growth of the photosynthetic biofilm collected from site when compared to growth in BG-11 media alone. There is a relatively linear correlation between FRD addition and the resulting biomass growth after 4 weeks (Supplementary Figure S1). The peak enrichment factor (FRD doped at 4.75 g/L) was shown to increase the biomass by a factor of ca. 25 times relative to just BG-11 (0.2 g/L biomass).

3.2 Microbial population change

The addition of an increasing amount of FRD material as a co-substrate was shown to have an increasing impact on the microbial populations sampled from the different systems at the cessation of the experiment. The dominant microbes remained the same irrespective of the differing amount of FRD added, though the abundance of the different species increased with the 'environmental pressure' of the added material (Supplementary Figure S2). The increase in FRD allowed some of the smaller populations of microbes to become better established, potentially creating an environment for greater diversity of metabolic activity. Phylum level observation (Supplementary Figure S8) showed that without the addition of any kimberlite, cyanobacteria (~75%) and Proteobacteria (~20%) dominated the microbial population. When kimberlite was added Bacteroidota, Chloroflexi, Gemmatimonadota, and Planctomycetota were all shown to better establish themselves in the culture systems.

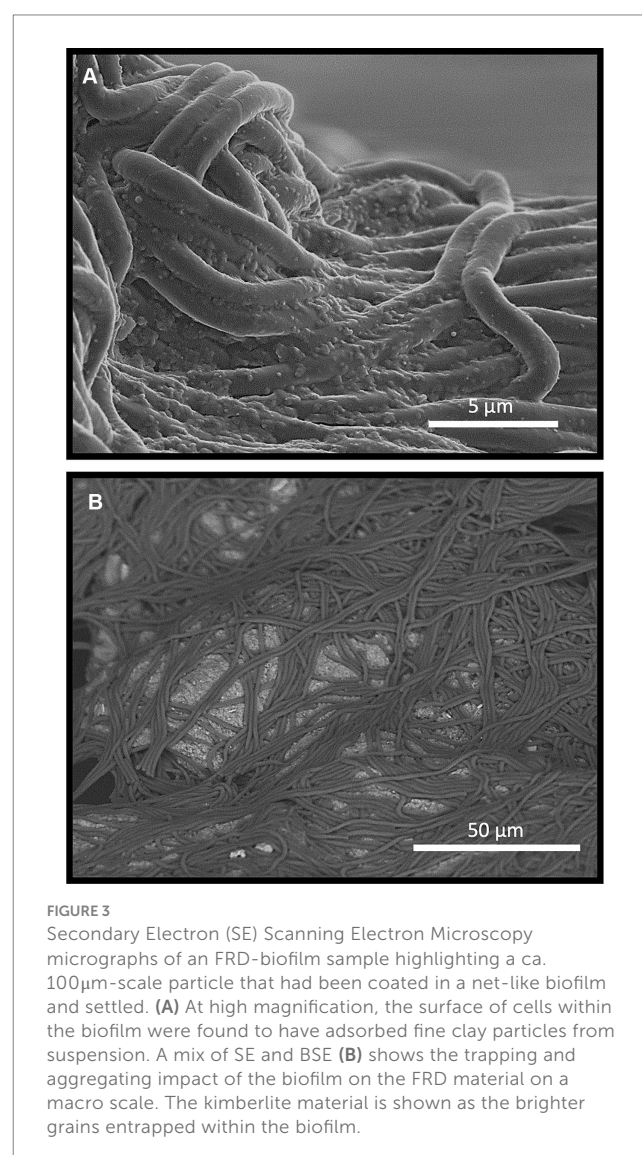## 3.3 The effect of FRD on dewatering/ settling

The addition of biofilm to an FRD slurry produced a slight improvement in the initial settling of suspended particles with no prior inoculation time (Supplementary Figure S3A). In contrast, when exposed to kimberlite over a 14-day inoculation period (Supplementary Figure S3B) accelerated settling was observed. The clarification of the slurries via microbial inoculation (10 cc and 20 cc) after 7 days are shown compared to the control at the cessation of the experiment with no inoculation time (Supplementary Figure S3). An accelerated settling rate of the fines was increased with the addition of more biofilm, with the 20 cc microbial additive (14-day inoculation) achieving the same level of clarification after 3 h (OD = 0.22) that was seen after 7 days in the control. Secondary electron SEM of the 100 μm scale grains, constituting ca. 90% of FRD by mass, demonstrated that they became rapidly coated in biofilm, and settled to the bottom of the graduated cylinder. In contrast, the residual clay fraction (10% by mass) slowly adsorbed to the cell envelopes, i.e., settling over days (data not shown).

3.4 Microbe – mineral composites under FRD settling conditions

The control system (FRD + water) produced a highly regular, repeating system typical of a sedimentary fining-upward sequence (Figure 4). The fine clay minerals are the last to settle, creating a less permeable boundary between each deposition cycle (Figures 4B,C) - effectively 'locking' the underlying sediment away from the above environment and atmosphere. In contrast, the Venetia microbes produced a significant macroscopic impact on the Venetia FRD, producing significant complex microbe-mineral interactions that were clearly visible on a system-wide scale (Figure 4D), after the 6-month experiment. The small initial inoculum survived repeated burial with FRD material, with the light-gradient environmental pressure driving the upward growth of the biofilm. This microbe-mineral mixing (growth characteristic) caused significant intra-layer and inter-layer mixing (homogenization of coarse and fine grains in each layer) (Figures 4E,F).

SEM imaging of FRD-biofilm growth experiment shows that the incorporation of biofilm into FRD produced aggregates involving relatively large particles and layers of biofilm (Figures 3A,B). Backscatter SEM of these materials confirmed that the larger (i.e., 100's of μm) sized particles had become netted in biofilm, forming tight aggregates (Figure 3B and as described in section 3.3) while the

FIGURE 3
Secondary Electron (SE) Scanning Electron Microscopy micrographs of an FRD-biofilm sample highlighting a ca. 100 μm-scale particle that had been coated in a net-like biofilm and settled. **(A)** At high magnification, the surface of cells within the biofilm were found to have adsorbed fine clay particles from suspension. A mix of SE and BSE **(B)** shows the trapping and aggregating impact of the biofilm on the FRD material on a macro scale. The kimberlite material is shown as the brighter grains entrapped within the biofilm.
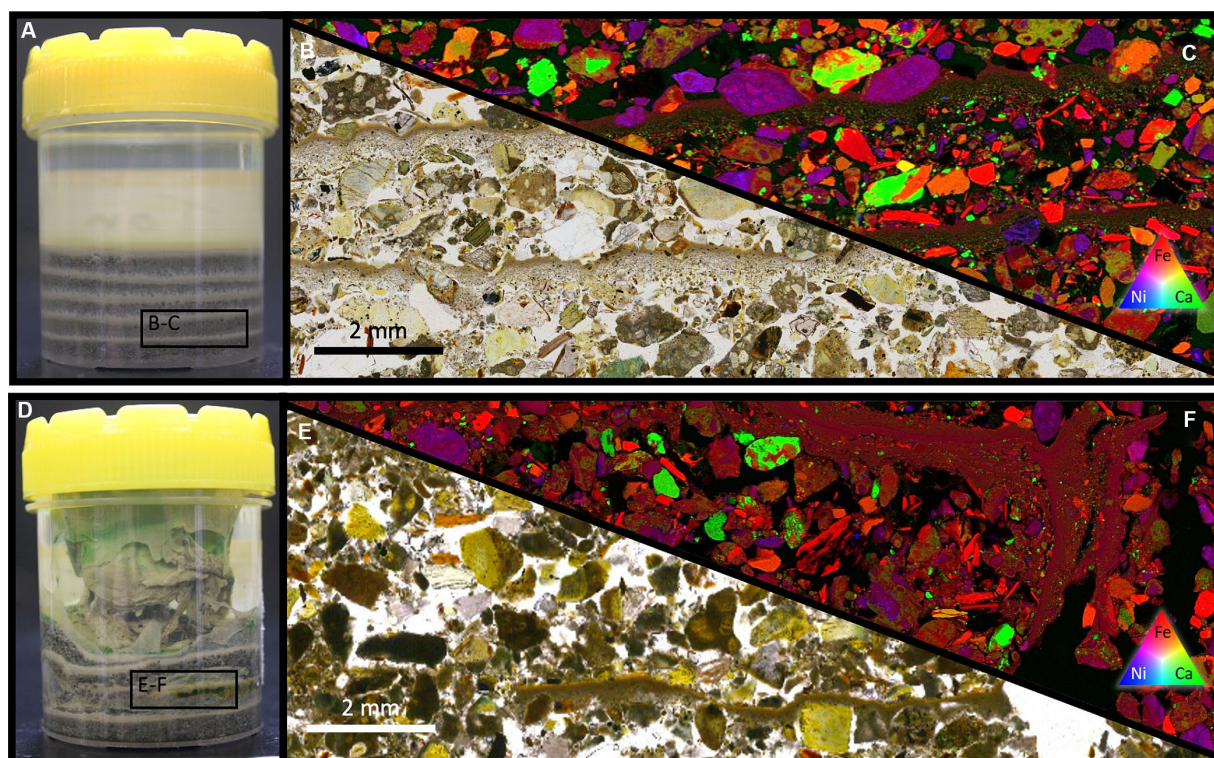
FIGURE 4
(A) A photograph of the control, repeated settling experiment. **(B)** PPL and XFM **(C)** of an embedded thin section of the control system showing the settling behavior of the FRD material resembling that of a repeating fining-upward sequence. Distinct size fractions are evident, with the bulk of the volume consisting of coarser FRD material whilst only a small portion is made up of fine material – consistent with the results of the grain size sorting via differential settling rates. **(D)** A photograph of the microbially inoculated composite experiment. **(E)** PPL and XFM **(F)** of an embedded thin section showing the physical intermixing within the sample. Fine and relatively coarse (100's of μm) particles are relatively well mixed with a lack of the repeated fining-up present in the control system.

finer clay particles are seen to be adsorbing/settling to the biofilm cell surfaces (Figure 3A).

4 Results Part B – field trial studies

4.1 Microbial aggregation and fines settling

Intermixing of the Venetia microorganisms and the FRD material accelerated the aggregation and settling of the fine material within the system. The control system (Figure 2D) showed no settling after 6 h (or ever) whereas the microbial system showed significant settling (Figure 2E). After 4-months uncovered incubation (which included multiple rain events), the inoculated system exhibited abundant, cm-scale biofilm on the FRD surface with no fines suspended in the water (Figure 2F) whereas the water atop the control system remained opaque due to the suspended fine-grained material (Figure 2G). After ~15 months both the systems had lost all overlaying water due to evaporation, though the material remained partially saturated (Figures 2H,I).

The inoculation of microbes into this settling process may be able disrupt the sedimentary sequence form when settling, and therefore maintaining a link between the sub-surface FRD and the atmosphere.

The mixing of a biofilm within the FRD material may also impact settling rates of the fine particles and the resulting de-watering processes. Water use and recycling is a heavily monitored aspect of all mining processes, even more so within diamond mining in the relatively water starved Southern Africa area.

4.2 Chemical analyses

The geochemical trends of the FRD material remained relatively similar in the experiments' surface samples over the duration of the experiment (Supplementary Figure S4). Ca, Fe, Mg, and P are shown to be relatively stable though all slightly decrease in wt.% suggesting that some weathering was occurring with the microbial treatment accelerating the wt. % decrease over the control. Water loss, i.e., evaporation, occurred over time in both systems and loss on ignition remained relatively unchanged. The geochemical trends over the depth of the system after 15 months show more variation (Supplementary Figure S5). Ca, Fe and Mg all decrease relative to $T = 0$ but with no significant change across depth. The decrease in Fe is consistent between the microbial and control system, though for Ca and Mg show a greater decrease in the microbially treated systems (consistent across depths) (Supplementary Figure S5). Al and Na are present in a higher wt. % in both systems relative to the $T = 0$ material, though are higher in the microbial systems. K and P are depleted in the microbial systems across all depths relative to $T = 0$, while are present in higher amounts (relative to $T = 0$) in the control. Water loss increased

significantly with depth, showing an increase from ~1 wt.% ($T=0$) to ~2 wt. % at surface, to an increase to ~5 wt.% at depth for both systems.

Total organic carbon analyses of the control and inoculated systems equalled 0.053 and 0.113%, respectively demonstrating that the inoculum represented 0.06% TOC. Using the mass of 685 kg kimberlite, and the mass of *Acidithiobacillus ferrooxidans* as a model weathering bacterium (Enders et al., 2006), the biologically treated

FRD was inoculated with 5.1×10^8 bacteria/ g FRD. After 15-months, the TOC of the control and inoculated increased and converged to 0.428% and 0.423, respectively.

## 4.3 Surficial carbonation – microbial initiation

XFM analysis of a cemented, microbially treated FRD sample collected at 8 months, demonstrated the establishment of carbonate pockets in association with biofilm (Figure 5A). The largest carbonate precipitates were observed at the FRD surface, though smaller, sporadic mineralized pockets of growth were observed below, but within a few cm of the FRD surface. All carbonate clusters are spatially associated with biofilms (draping textures, micro-fossils). High-resolution XFM (Figure 5B) and BSE SEM (Figure 5C) of a mm-scale carbonate cluster exhibit numerous nucleation points, though the extent of any accelerated weathering is difficult to ascertain due to the small particle size of the FRD materials. Secondary carbonates were not able to be observed with SEM in the control system.

4.4 Carbonate

In-situ carbonate wt.% within the FRD material was measured using MLA. Calcite and ankerite were combined as calcite within the systems to track the total changes in carbonate across the different layers after 15 months (Figure 6). MLA analysis recognized small amounts of ankerite across the system, though as these minerals were unable to be discernibly recognized using XFM and SEM (and as the
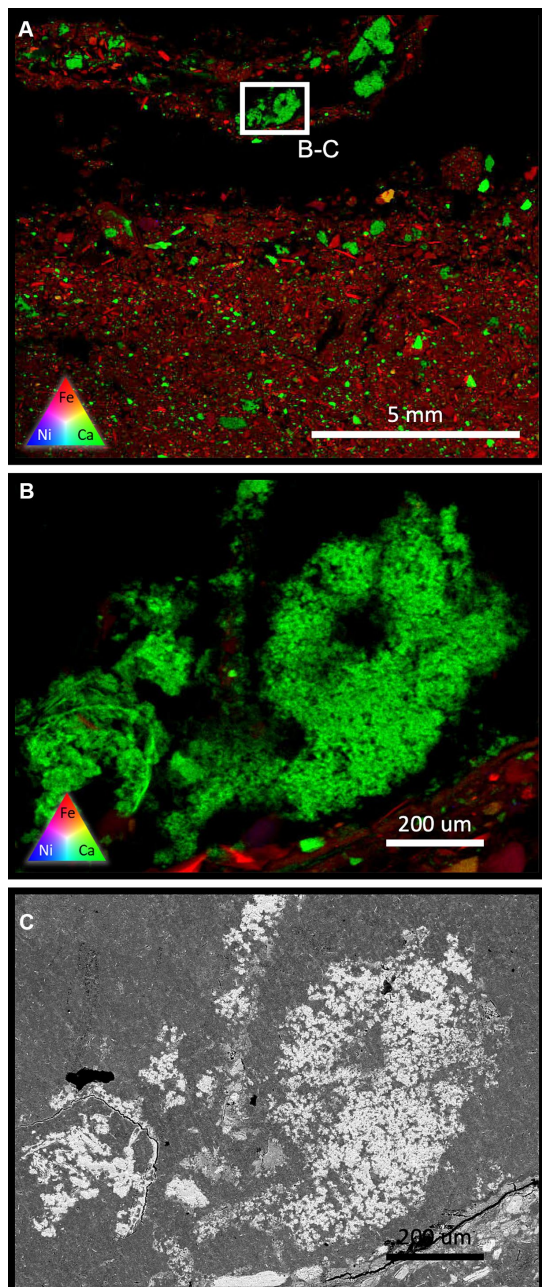
FIGURE 5
(A) An XFM scan of a relatively cemented surface sample from the microbially treated FRD system after 8 months. Areas showing young carbonate precipitation/cementation are visible in spatial association with draping textures, indicating a microbial presence. High-resolution XFM **(B)** shows the calcium dominated microbial carbonate contains multiple (hundreds) of micron-scale, individual nucleation points that have congregated, forming micro-cements. This texture is shown using BSE-SEM in tile **(C)**.
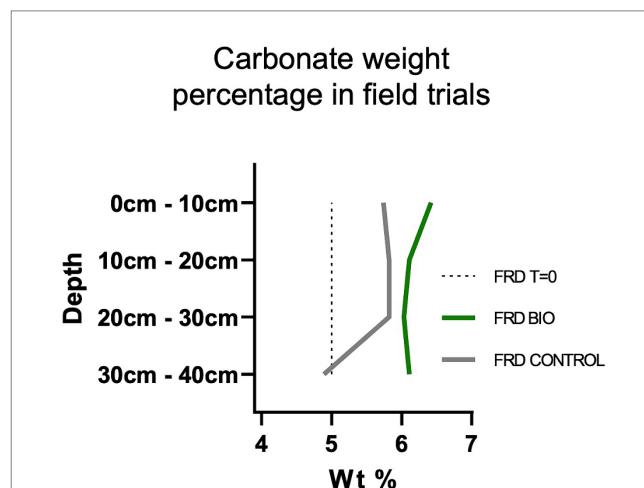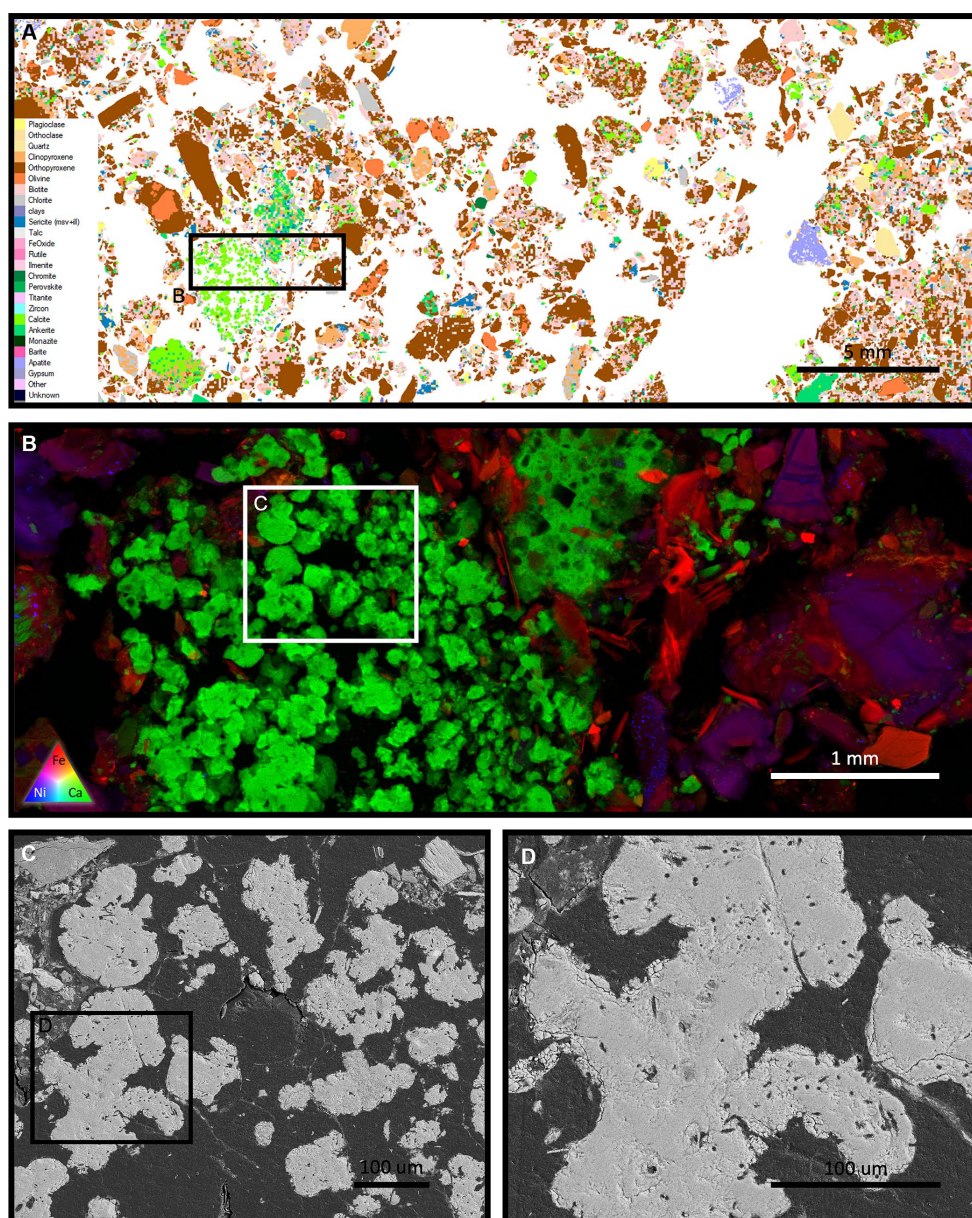

FIGURE 6
MLA derived *in-situ* carbonate wt. % (calcite + ankerite) across the FRD (bio + control) depth profiles. The microbial treatment resulted in a higher wt. % of carbonate across the entirety of the system relative to the control system and the $T = 0$ kimberlitic material. The highest wt. % of carbonate was observed at surface condition, which was ~1.5% (6.42 wt. % total) higher than the $T = 0$ material after 15-months. The control system increased the carbonate 0.74 wt. % at surface (5.74 wt. % total). At depth (30 cm – 40 cm), the gap between the systems becomes most apparent, with the microbial system allowing the carbonate to remain at ~6.1 wt. % (~1.1 wt. % above $T = 0$), whilst the control system allowed for the dissolution of carbonate to ~4.9 wt. % (a decrease of 0.1 wt. % relative to $T = 0$).

CDR potential between calcite and ankerite is similar) quantification and associated imaging was performed using calcite and referred to as 'total carbonate'. The total carbonate within the non-inoculated control system increased 0.7 wt.% at surface conditions. This increase was more than doubled with the addition of microbes, which drove up the carbonate by 1.42 wt.%, to a total of 6.42%. In the underlying layers (between 10 cm and 30 cm) the carbonate values converged slightly, though the microbial system always remained ~0.25 wt.% greater than the control. The largest discrepancies are found at the deepest layer of the system (30 cm – 40 cm), where the control system shows a carbonate depletion of 0.1 wt.% relative to $T = 0$, while the microbial system maintains a carbonate value of ~6.1 wt.% (~1.1 wt.% higher than $T = 0$) (Figure 6).

4.5 Later-stage mineral weathering and carbonation

MLA mapping of the inoculated FRD system after 15 months shows the development of relatively large secondary carbonate minerals (Figure 7A). This carbonate, unlike like that observed in the 8-month sample (Figure 5), grew at depths up to 20 cm, without

FIGURE 7
(A) An MLA scan showing the microbially treated FRD system after 15 months (10 cm − 20 cm horizon). Large pockets of newly formed secondary carbonate are present throughout the system, one of which is highlighted using XFM in tile **(B)**. This mm scale carbonate contains numerous individual nucleation sites, with a general trend showing larger minerals toward the centre. Assuming similar rates of mineral growth, this indicates different mineral ages within the system. BSE SEM **(C,D)** shows a high density of microbial fossils within the carbonate and intergranular branches, which are remnants of an encompassing biofilm that was present during carbonate growth.

access to sunlight and in a space limited environment. Observations via XFM show that this multi-mm scale carbonate cluster is made up of numerous individual carbonate minerals, nucleating individually and converging through continued growth (Figure 7B). All these carbonates are populated with extensive microbial fossils, observed using BSE SEM (Figures 7C,D) indicating their involvement in the nucleation and growth of these minerals. Intergranular cements were also observed throughout the carbonate cluster, linking the minerals (Figure 7C). This is indicative of the presence of an extensive biofilm that, based on the extent of branching within the carbonate, was spatially associated with carbonate growth with biofilm growing out from the carbonate mineral surfaces. This cluster shows the progressive development of carbonate and different generations of growth via the presence of different sizes of carbonate minerals within the same cluster, with the larger minerals occurring toward the middle of the cluster, getting smaller in size toward the outer regions. Assuming a generally consistent growth rate, this indicates that the cluster was growing outwards, enveloping the surrounding primary minerals, demonstrating its potential for creating an intergranular carbonate cement.

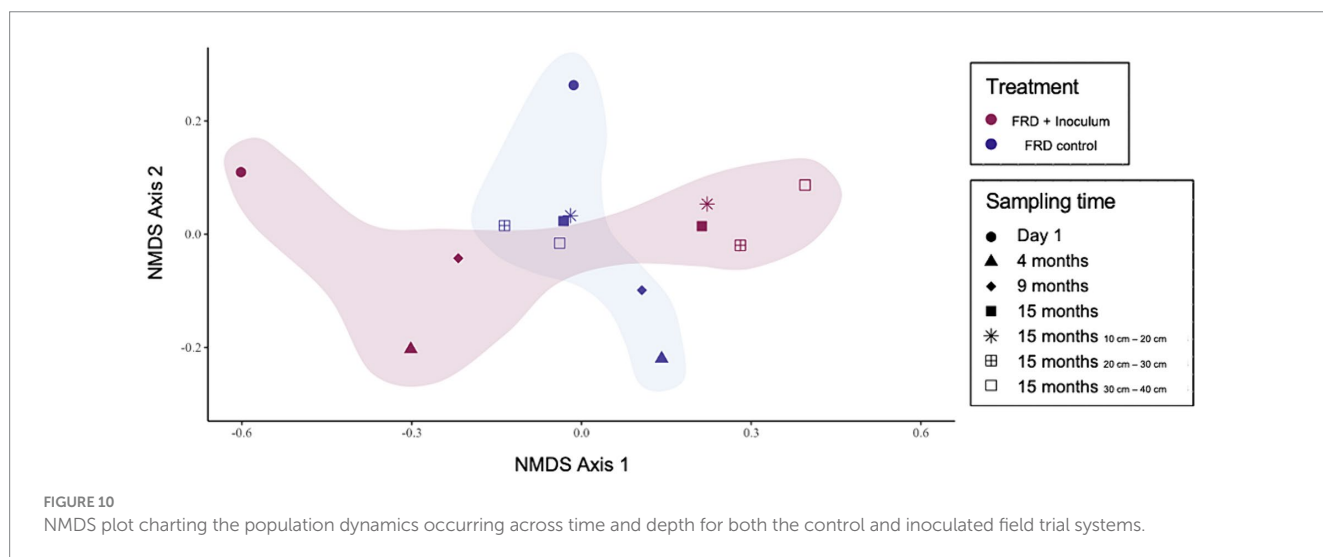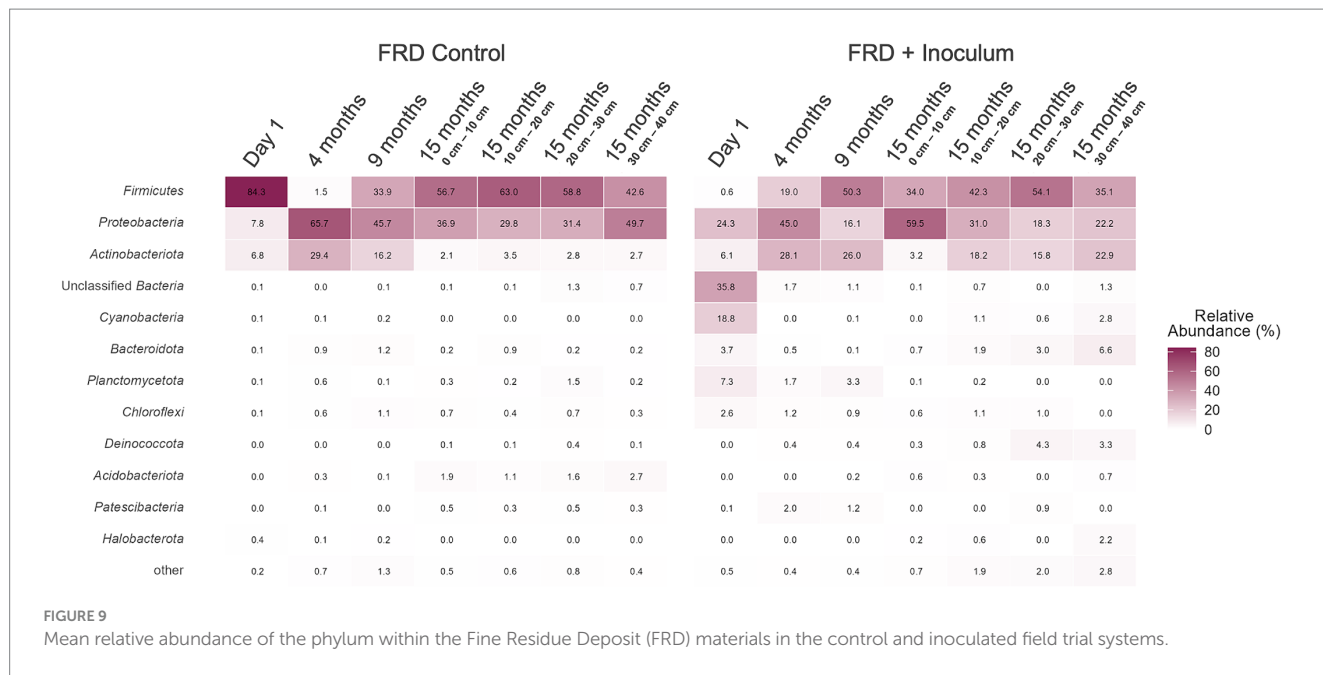## 4.6 Physical impact of microbes on FRD material

MLA and XFM analysis of the deepest section of the FRD systems demonstrate the impact that the addition of microbes into these environments (Figure 8). The control system (Figure 8A (MLA) and B (XFM)) shows the FRD as being highly homogeneous across the sample, representing a highly impermeable substrate; a negative quality in terms of producing mineral carbonation using atmospheric CO_2. The addition of microorganisms (Figure 8C (MLA) and D (XFM)) heavily partitioned the FRD substrate by aggregating the finer material and clumping it together, leaving the larger grains free of fine intergranular material. This produced an environment with a higher degree of porosity and permeability, two essential traits for allowing atmospheric CO_2 to flux into the system.

4.7 Biosphere

The inoculated system was dominated by Cyanobacteria and Proteobacteria at $T=0$, though the microbiome shifted for the
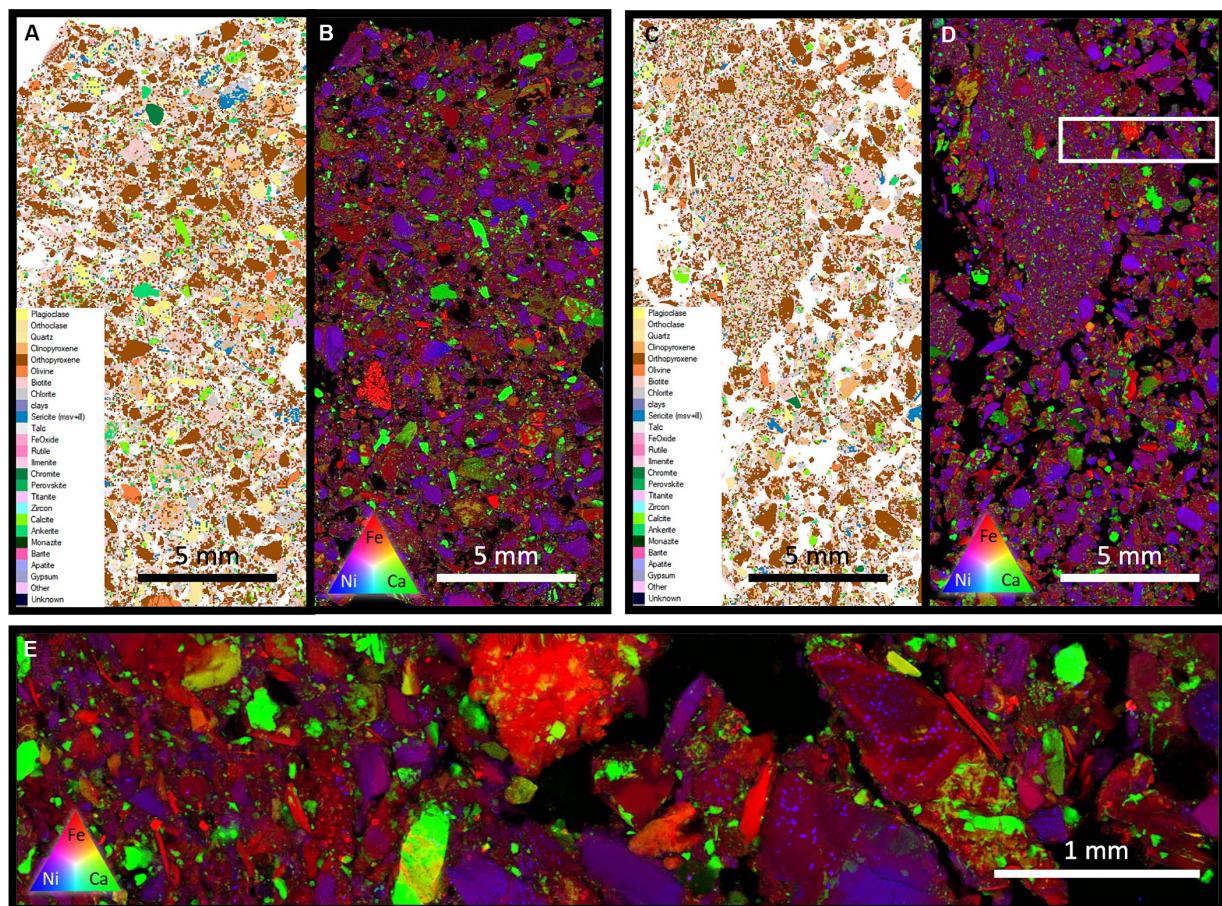
FIGURE 8
Samples from the deepest sections of the FRD systems (30 cm – 40 cm). MLA **(A)** and XFM **(B)** of the control system shows a high degree of homogeneity throughout the environment, with a low degree of sorting. The system with the microbial addition (MLA-C, XFM-D) show a highly partitioned system, with the fine material aggregated and separated from the larger grains. High-resolution XFM across the transition from the fine grain area to the large grain area shows no change in mineral composition, indicating that this partitioning was induced by other factors, possible the influence of microbes.

FIGURE 9
Mean relative abundance of the phylum within the Fine Residue Deposit (FRD) materials in the control and inoculated field trial systems.

FIGURE 10
NMDS plot charting the population dynamics occurring across time and depth for both the control and inoculated field trial systems.

remainder of the experiment – with the Proteobacteria remaining a dominant phylum though with Firmicutes and Actinobacteria developing major populations for the remainder of the experiment (Figure 9). The uninoculated (native control) system showed little to no presence of cyanobacteria throughout the experiment, though, much like the inoculated system, housed a microbiome dominated by Proteobacteria, Firmicutes, and Actinobacteria (Figure 9).

At the genus level, microbes present at time of inoculation were ubiquitously replaced after 4 months and were not seen to return in any significant way (Data not shown). Originally dominated by *Rhodobacter* and *cyanobacteria*, the population shifted toward a biome primarily containing *Bacillus* and *Pseudomonas*, both of which were present both at surface and depth throughout the remainder of the experiment. The uninoculated system was initially dominated by *Bacillus* and *Planococcus*, the first of which remained a prominent part of the biome throughout the experiment at surface

and shallow conditions. The *Planococcus* sp. was not present after the first 4 months, after which the biome became primarily populated with *Luteimonas* sp. (4 months) and *Pseudomonas* sp. (8 months). A small proportion of a *Desulfosporosinus* sp., a known anaerobic sulphate-reducing microorganism, was observed at depth after 15 months.

The conditions created in the deeper sections of the control experiments allowed for the development of a relatively large population of Acidobacteriota. This group of microbes are only seen in the control system after 15 months.

The microbial population dynamics within these field trial systems were investigated via the use of an NMDS ordination analysis (Figure 10). The large disparity between the microbiomes was expected at the start of the experiment. Throughout the field trial, the environmental pressure applied to the microbial communities by the kimberlitic material worked to converge the population before another

slight separation after 15 months. As expected, depth played a determining role in the population make-up of the microbes throughout each system, though to a lesser degree than time. This is demonstrated in Figure 10, with the samples collected across the depth profile showing a more tightly bound grouping than the samples collected over the duration of the experiment.

5 Discussion

5.1 Microbial-mineral interactions

The reciprocal impact of the kimberlite on the microbes and vice versa was shown across the lab and field scale aspects of this investigation, and via the varied analytical approaches, this interaction can be seen at both micro and macro scales. The continual biogeochemical breakdown of the kimberlitic material by the microbial consortia created a positive feedback loop within the environment – with the growing biomass allowing for a greater release of cations (due to bio-weathering) over time. This increase in cations allowed for both the continued growth of micro-organisms in the system, along with the enhanced bio-precipitation of secondary carbonate mineralogy, creating a relatively self-sustaining, carbon sequestering, process. The laboratory model provided evidence of enhanced weathering, nutrient acquisition, bacterial growth, materials handling (inoculation and settling) and mineral carbonation, supporting a next stage TRL 6 pilot demonstration in an operational environment.

5.2 Water-rock interactions supporting growth

The enhanced growth of biofilm by the addition of FRD kimberlite under laboratory conditions was remarkable, achieving a 25X increase in biomass production after 4 weeks incubation (Supplementary Figure S1). Growth intuitively requires weathering, corresponding to an enhanced phosphorous availability, a typical limiting nutrient in most environments. The release of essential trace elements, such as iron and nickel, also aid in growth via the support of enzyme function (Banfield et al., 1999).

The increase in biofilm production served a range of purposes; supporting the long-term goal of creating a carbon neutral mine via mineral carbonation by enhanced capture of CO_2 into biomass; production of bioweathering microorganisms – catalyst (Supplementary Figure S2); and mineral carbonation under surficial and burial conditions. The growth supporting ability of kimberlite was observed within the field trial study via the development of TOC in both the control and inoculated system. The large increase in TOC after 15 months is consistent with the kimberlite providing nutrients supporting the growth of bacteria (Supplementary Figure S1) as well as driving the biology, i.e., the selection of kimberlite specific bacteria (Figure 9; Supplementary Figure S2). The active production of biomass (OC) suggests that inoculation may not be required for kimberlite weathering (bacterial growth) to occur, though the system did not produce a corresponding increase in mineral carbonation. The production of biomass and competition for nutrients would have

likely produced a corresponding increase in cell death and respiration, i.e., carbonic acid formation, which would have limited carbonate precipitation.

5.3 Microbial response to kimberlite

The addition of kimberlite as a co-substrate and growth additive, promoted the diversification of the microbial population under laboratory conditions. This is due to the change in environmental inputs, materials presented to the consortia, both in term of chemistry (increased nutrients), and substrate (higher surface area and water-rock interactions, which support the growth/development of microorganisms). The increase in biodiversity, away from being dominated by cyanobacteria (Supplementary Figure S2) was expected as the opportunity for additional metabolic processes, e.g., chemotrophy and lithotrophy, which occurred with the addition of FRD (labile, ultramafic material). The environmental selective pressure provided by the presence the kimberlite worked to diversify the microbial population, the metabolic pathways being used and as a result, expanded the impact the microbes had on the kimberlite.

5.4 Dewatering and settling

The addition of FRD to water under mine site or laboratory conditions creates a cloudy suspension of clays producing a dewatering process challenge. Disposal of FRD material in large, repeated layers (100's of mm) creates a series of relatively impermeable layers due to the repeated settling of fine clay-sized (and clay) minerals (Wang et al., 2014). Once formed, these layers were observed to act as aquifers, preventing the movement of water through the layer. This layering both limits the natural weathering throughout the FRD and disconnects the underlying FRD material from the atmosphere (CO_2 source). The abiotic dissolution of silicate minerals (such as olivine) can also result in the formation of amorphous Si layers and Fe (III) oxide precipitates, both of which can further imped underlaying mineral dissolution. These layers have been shown to be susceptible to microbial weathering, which can remove developed layers and prevent their development, allowing for continued mineral dissolution (Pokharel et al., 2019; Gerrits et al., 2020). Inoculation of the kimberlitic material to create a FRD-biofilm composite, is essential to both enhance weathering, enhance mineral carbonation and to aid in dewatering via clay adsorption. The adsorption of clays to biomass, promoting dewatering, was observed under three conditions: 1. In the layered FRD culture system (Figure 4); 2. In the biomass culture experiment (Supplementary Figure S1); and 3. In the settling experiment (Supplementary Figure S4).

Given the scale of the Venetia Mine, producing 4.74 MT of processed kimberlite annually (Mervine et al., 2018), and the necessary production of an FRD composite being critical to enhance weathering, inoculation of the <800 μm grains would be an ideal processual outcome. This may be most readily achieved by the FRD enhanced production of biomass followed by the addition of this biomass to the mine site FRD dewatering process

stream immediately before disposal to the tailings dam, allowing all the FRD materials to be inoculated before disposal. Mixing biofilm with the FRD suspension will produce a composite of clay-coated bacteria + bacteria coated grains, disrupting the layering which occurs during abiotic disposal, preventing the formation of clay layers, which serve as barriers to weathering and mineral carbonation.

5.5 Geochemistry and biogeochemical cycling

The geochemistry of the field trial systems after 15 months reveals evidence of chemical cycling through the environment. The general trend of depleted relatively mobile elements (Ca, Fe, Mg) and an increase in wt% of relatively immobile elements such as aluminium shows evidence for the weathering of the FRD material (Supplementary Figure S4). This breakdown of the primary mineralogy is not easily observed using *in-situ* observation (XFM, MLA) due to the fine grain size. The chemistry of the inoculated system indicates a higher degree of weathering as compared to the control due to the greater levels of change relative to the $T = 0$ material, showing that the introduction of the Venetia microbes into the FRD material hastens mineral breakdown. This results in a higher corresponding level of carbonate precipitation within the biogenic system as there is a higher amount of cations (Ca, Fe, Mg) being released from the primary mineralogy. Potassium, an element essential for microbial/plant growth (Wang et al., 2015; Ahmad et al., 2016) was readily consumed for its vital role in metabolic processes, being depleted in the biogenic system after 15 months, relative to both the starting material and the control.

5.6 Microbial impact on carbonate

Biogenic carbonate was first observed within the inoculated system after 8 months in the form of a small, cemented block on the surface of the field trial system. This carbonate was spread through the surface section, though always in close spatial association with biofilm, and only grew to a significant size (100's of μm) at near surface conditions (Figure 5). The surface confinement of the carbonate growth is an effect of both preferential growth in that specific environment, along with the lack of spatial pressure that negatively impacts growth deeper within the material.

After 15 months, the reach of the large-scale carbonate growths had extended to the deeper parts of the system, where mm scale carbonate growths are shown enveloping large areas of FRD material (Figure 7). The high surface area of the FRD material provides ample substrate for nucleation points, and as such, any correlation between areas of higher mineral degradation and abundance of carbonate growth is hard to ascertain. The evidence of microbial carbonate at depth is important as it was shown that when the FRD was not inoculated, conditions were such that carbonate wt. % decreased below 30 cm (Figure 6). This is feasibly due to the growth of Acidobacteriota in the control

system. This contrasts with the inoculated material which saw no growth of the Acidobacteriota - maintaining an increased level of carbonate generation relative to the upper layers (Figure 6).

The overall trends seen throughout this biogenic system is one of gradual cementation of the FRD minerals at both surface and sub-surface conditions, indicating the presence of multiple biogenic pathways for carbonation. Multiple pathways indicate that different groups of microbes can facilitate carbonate precipitation as the environment changes within the system, with the changes being driven by depth and resulting in the loss of light and atmospheric connectivity. These changes manifest in population shifts within the system as shown in Figures 9, 10. This data shows an immediate move away from the inoculated population due to environmental pressure from the kimberlite, and the conditions set by the fine-grained material. This is evident as the microbial shift observed within the inoculated system moves toward the microbiome already present in, and further promoted by, the kimberlite material (Figures 9, 10). The dominant microbes in the inoculum ($T = 0$) (cyanobacteria, *Rhodobacter* sp., *Porphyrobacter* sp.) are either not present, or made up an insignificant percentage of the control (natural) microbiome, though the bacteria that start to populate the system after experiencing the kimberlite driven environmental pressure are the same seen in the control system (Figure 9).

The microbial richness at the start of the field trial experiments was more than 5X higher in the inoculated system than the control (Supplementary Figure S6). This is undoubtedly a strong driver of biogeochemical cycling and the eventual carbonation of the kimberlite material. Though, based on the convergent nature of the microbial populations, it appears that the microbial population that is inserted into the material matters less than the overall increase in biomass or perhaps the existence of a complex biosphere. The inoculation of the FRD provided a 'microbial kickstart' to the weathering and secondary precipitation in the system, while preventing the growth of carbonate limiting organisms (Acidobacteriota, Figure 9).

5.7 Potential for mine emission offsets

The ~1.5 wt.% increase in carbonate values (calcite + ankerite; MLA) relative to the starting material (and 0.7 wt.% higher than control) across the top 10 cm of the FRD profile demonstrates that there is a near surface catalyst enhancing mineral carbonation; the compounding influence of both the increased microbial activity and proximity to atmospheric CO_2. A 1.5 wt.% increase in calcium carbonate within this FRD system shows that 6.6 g CO_2e/kg of kimberlite has been sequestered. If this 1.5 wt. % (adjusted to 1.2 wt.% over 12 months) benchmark could be achieved across the Venetia mine treated ore (4.74 Mt. in 2016) (Mervine et al., 2018), this would equate to the sequestration of ~25,024 T of CO_2e within the mined material every year – correlating to an offset in mine emissions of 11.92% (using the rate of carbonation adjusted to annual sequestration). The control system was also shown to sequester CO_2, a projected ~11,836 T of CO_2e. This corresponds to a 5.62% offset in mine emissions, when left to weather naturally without a microbial boost.

5.8 Rate of carbonate vs. historically mined kimberlite material

The process by which microorganisms accelerate the sequestration of atmospheric carbon within crushed kimberlite material mimics the natural transition that takes place in the transformation of blue ground to yellow ground kimberlite at surface conditions. The rate of this transformation is impossible to determine in historical kimberlite residue, though sample core would be interesting to study. However, by analysing future mine site FRD residue, our estimates may become more robust and the rate of change / mineral carbonation potential can be estimated.

Mined kimberlite material from the Cullinan diamond mine in Gauteng, South Africa, developed an inter-granular carbonate cement over a ~ 50-year period (Jones et al., 2023c). This kimberlite was extracted for mining from a depth that had not allowed for weathering to occur, though the secondary carbonate within the mined Cullinan material had developed over time to account for 16.39 wt.% of the cemented kimberlite system. This historical system contained a coarser grain size (Coarse Residue Deposit; CRD) and was stored in large piles, allowing it to dry and retain the void space needed for vadose exchange. Assuming a constant growth rate of the carbonate in the Cullinan material, and that like Venetia, it contained ~5 wt.% primary carbonate, this indicates that within the Cullinan mined material, secondary carbonate increased annually by ~0.228 wt.%. Using this rate estimate, the addition of microbes into the FRD material at surface conditions were able to produce secondary carbonate at a rate ca. 5 x that seen within the Cullinan mined material. Note, microbially induced carbonate precipitation (MICP) will not only be a method for on-site carbon sequestration but will have on going effects on tailings stabilization and soil regeneration.

6 Conclusion

Microbial consortia, originally sampled from the Venetia diamond mine in South Africa, was shown to have a profound effect on the transformation of Venetia FRD blue ground material into early-stage yellow ground. Exploratory studies undertaken under laboratory conditions reveal the impact that kimberlitic material has on mine-soured biofilms, and vice versa. Kimberlitic material had impacts on microbial growth and developing consortium richness, while being aggregated and heterogenized by the microbial inoculation. Expanding into field trials, the population biodiversity was again heavily impacted by environmental pressure exerted by the kimberlite after the initial inoculation, pushing the biome toward organisms seen in the natural control system, though at a much higher overall biomass. This microbial effect first presented via the aggregation of the fine particles during deposition, resulting in accelerated settling and dewatering. This aggregating effect, spreading throughout the system during the experiment, created a relatively partitioned, well-drained, but still 'wet' environment compared to the control, which is ideal for mineral carbonation (Harrison et al., 2014). This partitioning also meant that the more of the kimberlite (carbonation host) was exposed to the atmosphere (carbon source) through the eradication of the impermeable layers created when the fine clay particles are left to settle without the biological influence. This physical manipulation, along with the increased microbial activity, produced biogenic carbonate throughout the entirety of the 40 cm deep field trial study. This carbonate was shown

to be spatially associated with biofilms, have numerous nucleation points, and contain fossilized microbes. The mineral carbonation seen at surface conditions occurred at a rate roughly 5 x faster than carbonation measured in historically mined CRD kimberlite, and twice the rate of the FRD control system. When extrapolated to match the amount of ore treated annually, this equates to a mine emission offset of nearly 12% per annum. Biologically accelerated mineral carbonation within mined kimberlitic material has been shown to be potentially successful, simple, and hands-off approach to accelerating the passive sequestration of CO_2.

Data availability statement

Microbial data is stored in the BioSample database (NCBI); ascension number PRJNA1128813.

Author contributions

TJ: Conceptualization, Data curation, Formal analysis, Investigation, Methodology, Project administration, Software, Validation, Visualization, Writing – original draft, Writing – review & editing. JP: Data curation, Formal analysis, Methodology, Writing – review & editing. AlL: Data curation, Software, Supervision, Writing – review & editing. Gd: Data curation, Formal analysis, Methodology, Writing – review & editing. SG: Formal analysis, Investigation, Visualization, Writing – review & editing. BR: Investigation, Methodology, Software, Visualization, Writing – review & editing. AV: Conceptualization, Investigation, Methodology, Writing – review & editing. AnL: Data curation, Formal analysis, Investigation, Methodology, Resources, Software, Visualization, Writing – review & editing. GS: Conceptualization, Data curation, Funding acquisition, Investigation, Methodology, Project administration, Resources, Supervision, Visualization, Writing – review & editing.

Funding

Conflict of interest

The authors declare that the research was conducted in the absence of any commercial or financial relationships that could be construed as a potential conflict of interest.

The author(s) declared that they were an editorial board member of Frontiers, at the time of submission. This had no impact on the peer review process and the final decision.

Publisher's note

All claims expressed in this article are solely those of the authors and do not necessarily represent those of their affiliated organizations, or those of the publisher, the editors and the reviewers. Any product that may be evaluated in this article, or claim that may be made by its manufacturer, is not guaranteed or endorsed by the publisher.

Supplementary material

The Supplementary material for this article can be found online at: https://www.frontiersin.org/articles/10.3389/fclim.2024.1345085/full#supplementary-material

SUPPLEMENTARY FIGURE S1
A plot of extra biomass (g/L dry weight) produced with the addition of kimberlite as a nutrient supplement. The non-FRD BG-11 control, equaling 0.17 g biomass was subtracted from each value to zero the origin.

SUPPLEMENTARY FIGURE S2
Mean relative abundance of the 11 most abundant genera (or lowest resolved taxonomic level) with an abundance of 3% or more showing the population shifts brought upon by the addition of kimberlite as a co-substrate. As more kimberlite is added to a growth system, a higher degree of diversity was promoted.

SUPPLEMENTARY FIGURE S3
Settling properties of FRD-biofilm composites. Two settling experiments showing the acceleration of material aggregation with no inoculation time (I = 0) **(A)** and with 14 days incubation (I = 14) **(B)**. The variability in the first few

hours (I = 0) corresponded to biofilm-FRD composite settling, versus floating biomass via gas production, versus biofilm colonising the sides of the graduated cylinder (settling vessel) as adsorbed biofilm. The impact of biofilm amendments to FRD settling was measured using optical density (OD600 nm). These OD results are averaged from both the surface and depth samples, all of which were run in duplicate. All microbial treatments accelerated the settling of the fine particles, though allowing a 14-day inoculation period increased the effectivity of the microbial additive. There was not a distinct difference in settling rates between the differing amounts of microbes added when deprived of a inoculation period **(A)**, though allowing time for the microbes to inter-mingle with the material shows **(B)** reveals that there is an increase in settling acceleration with an increase in microbial inoculation. Photographs of the settling experiment: control, 10 cc, and 20 cc show these treatments after 7 days (I=0). The extent of water clarification is evident, with the control appearing cloudy, whilst the 20 cc system is shown to the relatively clear.

SUPPLEMENTARY FIGURE S4
Major oxides sampled from the surface (0 – 10 cm) of the FRD field trial systems over 15 months (01/2020 – 04/2021). Ca, Fe, Mg, and P are shown to be relatively stable over the 15-month experiment – all slightly decreasing in wt.%, though the microbial treatment accelerating the decrease over the control. Al and Na have very similar trends, increasing in wt.% for 10 months, before leveling off and slightly decreasing. The H2O loss over time increased in both the bio-treated and control system (both ~ 1 wt.%), possibly indicating a widespread hydration of clay minerals. Loss on ignition remained relatively constant.

SUPPLEMENTARY FIGURE S5
Major oxides sampled across four depths from the FRD field trial systems after 15 months. Ca, Fe and Mg are shown to have been partially weathered out of the system – more so with the microbial addition (vs control) for Ca and Mg, less so for Fe. The Al wt. % increased due to its relative immobility in soil. P and K in the microbial exp. are shown to have decreased over time, whilst increasing in the control – likely due to the uptake of the elements by the microbial community. Water loss increased with depth across both systems and loss on ignition remained constant.

SUPPLEMENTARY FIGURE S6
Alpha diversity indices of the control and inoculated field trial system.

SUPPLEMENTARY FIGURE S7
The initial microbiome collected from the Venetia pit.

SUPPLEMENTARY FIGURE S8
Phylum level abundance of the microbial biofilm with differing amounts of FRD amendment added as a co-substrate.

References

Ahmad, M., Nadeem, S. M., Naveed, M., and Zahir, Z. A. (2016). "Potassium-solubilizing Bacteria and their application in agriculture" in *Potassium solubilizing microorganisms for sustainable agriculture*. eds. V. Meena, B. Maurya, J. Verma and R. Meena (New Delhi: Springer).

Allsopp, H. L., Smith, C. B., Seggie, A. G., Skinner, E. M. W., and Colgan, E. A. (1995). The emplacement age and geochemical character of the Venetia kimberlite bodies, Limpopo Belt, northern Transvaal. *S. Afr. J. Geol.* 98, 239–244.

Anderson, P., and Christenson, T. H. (1988). Distribution coefficients of cd, co, Ni, and Zn in soils. *J. Soil Sci.* 39, 15–22. doi: 10.1111/j.1365-2389.1988.tb01190.x

Banner, J. L. (1995). Application of the trace element and isotope geochemistry of strontium to studies of carbonate diagenesis. *Sedimentol* 42, 805–824. doi: 10.1111/j.1365-3091.1995.tb00410.x

Banfield, J. F., Barker, W. W., Welch, S. A., and Taunton, A. (1999). Biological impact on mineral dissolution: application of the lichen model to understanding mineral weathering in the rhizosphere. *Procee. National Acade. Sci.* 96, 3404–3411.

Bodénan, F., Bourgeois, F., Petiot, C., Augé, T., Bonfils, B., Julcour-Lebigue, C., et al. (2014). Ex situ mineral carbonation for CO2 mitigation: evaluation of mining waste resources, aqueous carbonation processability and life cycle assessment (Carmex project). *Min. Eng.* 59, 52–63. doi: 10.1016/j.mineng.2014.01.011

Brandl, H., and Faramarzi, M. A. (2006). Microbe-metal-interactions for the biotechnological treatment of metal-containing solid waste. *China Particuology* 4, 93–97.

Callahan, B. J., McMurdie, P. J., and Holmes, S. P. (2017). Exact sequence variants should replace operational taxonomic units in marker-gene data analysis. *The ISME journal* 11, 2639–2643.

Coleman, H. T., Matthews, T. G., Sherman, C. D., Holland, O. J., Clark, Z. S., Farrington, L., et al. (2021). Contrasting patterns of biodiversity across wetland habitats

using single-time-point environmental DNA surveys. *Aquatic Conser. Marine and Freshwater Ecosystems* 33, 1401–1412.

Costa, O. Y., Raaijmakers, J. M., and Kuramae, E. E. (2018). Microbial extracellular polymeric substances: ecological function and impact on soil aggregation. *Front. Microbiol.* 9:337094. doi: 10.3389/fmicb.2018.01636

Dupraz, C., Reid, R. P., Braissant, O., Decho, A. W., Norman, R. S., and Visscher, P. T. (2009). Processes of carbonate precipitation in modern microbial mats. *Earth-Science Reviews* 96, 141–162.

Enders, M. S., Knickerbocker, C., Titley, S. R., and Southam, G. (2006). The role of bacteria in the supergene environment of the Morenci porphyry copper deposit, Greenlee County. *Arizona. Econ. Geol.* 101, 59–70. doi: 10.2113/gsecongeo.101.1.59

Field, M., Stiefenhofer, J., Robey, J., and Kurszlaukis, S. (2008). Kimberlite-hosted diamond deposits of southern Africa: a review. *Ore Geol. Rev.* 34, 33–75. doi: 10.1016/j.oregeorev.2007.11.002

Gadd, G. M., and Raven, J. A. (2010). Geomicrobiology of eukaryotic microorganisms. *Geomicrobiology Journal* 27, 491–451.

Gagen, E. J., Levett, A., Shuster, J., Fortin, D., Vasconcelos, P. M., and Southam, G. (2018). Microbial diversity in actively forming iron oxides from weathered banded iron formation systems. *Microb. Environ.* 33, 385–393. doi: 10.1264/jsme2.ME18019

Gerrits, R., Pokharel, R., Breitenbach, R., Radnik, J., Feldmann, I., Schuessler, J. A., et al. (2020). How the rock-inhabiting fungus K. petricola A95 enhances olivine dissolution through attachment. *Geochim. Cosmochim. Acta* 282, 76–97. doi: 10.1016/j.gca.2020.05.010

Harrison, A., Dipple, G., Power, I., and Mayer, K. (2014). Influence of surface passivation and water content on mineral reactions in unsaturated porous media: implications for brucite carbonation and CO2 sequestration. *Geochim. Cosmochim. Acta* 148, 477–495. doi: 10.1016/j.gca.2014.10.020

Howard, D. L., de Jonge, M. D., Afshar, N., Ryan, C. G., Kirkham, R., Reinhardt, J., et al. (2020). The XFM beamline at the Australian Synchrotron. *J. Synchrotron Radiat.* 27, 1447–1458. doi: 10.1107/S1600577520010152

Jones, T. R., Poitras, J., Gagen, E., Paterson, D. J., and Southam, G. (2023b). Accelerated mineral bio-carbonation of coarse residue kimberlite material by inoculation with photosynthetic microbial mats. *Geochem. Trans.* 24:1. doi: 10.1186/s12932-023-00082-4

Jones, T. R., Poitras, J., Levett, A., Langendam, A., Vietti, A., and Southam, G. (2023a). Accelerated carbonate biomineralisation of Venetia diamond mine coarse residue deposit (CRD) material–a field trial study. *Sci. Total Environ.* 893:164853. doi: 10.1016/j.scitotenv.2023.164853

Jones, T. R., Poitras, J., Paterson, D., and Southam, G. (2023c). Historical diamond mine waste reveals carbon sequestration resource in kimberlite residue. *Chem. Geol.* 617:121270. doi: 10.1016/j.chemgeo.2022.121270

Krumbein, W. E. (1974). On the precipitation of aragonite on the surface of marine bacteria. *Naturwissenschaften* 61:167. doi: 10.1007/BF00602591

Lackner, K. S. (2003). A guide to CO_2 sequestration. *Science* 300, 1677–1678.

Martin, M. (2011). Cutadapt removes adapter sequences from high-throughput sequencing reads. *EMBnet. journal* 17, 10–12.

Maschinski, J., Southam, G., Hines, J., and Strohmeyer, S. (1999). Efficacy of subsurface constructed wetlands using native southwestern U.S. plants. *J. Environ. Qual.* 28, 225–231. doi: 10.2134/jeq1999.00472425002800010027x

Masson-Delmotte, V., Zhai, P., Pirani, A., Connors, S. L., Péan, C., Berger, S., et al. (2021). Climate change 2021: the physical science basis. *Contribution of working group I to the sixth assessment report of the intergovernmental panel on climate change* 2:2391.

McCutcheon, J., Nothdurft, L. D., Webb, G. E., Shuster, J., Nothdurft, L., Paterson, D., et al. (2017). Building biogenic beachrock: visualizing microbially-mediated carbonate cement precipitation using XFM and a strontium tracer. *Chem. Geol.* 465, 21–34. doi: 10.1016/j.chemgeo.2017.05.019

Mervine, E. M., Wilson, S. A., Power, I. M., Dipple, G. M., Turvey, C. C., Hamilton, J. L., et al. (2018). Potential for offsetting diamond mine carbon emissions through mineral carbonation of processed kimberlite: an assessment of De beers mine sites in South Africa and Canada. *Mineral. Petrol.* 112, 755–765. doi: 10.1007/s00710-018-0589-4

Oksanen, J., Blanchet, F. G., Friendly, M., Kindt, R., Legendre, P., McGlinn, D., et al. (2019). Package 'vegan'. *Commun. Ecol. Package Ver.* 270, 4–6.

Paterson, D., Jonge, M.D.de, Howard, D.L., Lewis, W., McKinlay, J., Starritt, A., et al., (2011). The X-ray fluorescence microscopy beamline at the Australian synchrotron. *In AIP Conference Proceedings.* American Institute of Physics. 1365, 219–222.

Pokharel, R., Gerrits, R., Schuessler, J. A., and von Blanckenburg, F. (2019). Mechanisms of olivine dissolution by rock-inhabiting fungi explored using magnesium stable isotopes. *Chem. Geol.* 525, 18–27. doi: 10.1016/j.chemgeo.2019.07.001

Power, I. M., Wilson, S. A., and Dipple, G. M. (2013). Serpentinite carbonation for CO2 sequestration. *Elements* 9, 115–121. doi: 10.2113/gselements.9.2.115

Power, I. M., Wilson, S. A., Small, D. P., Dipple, G. M., Wan, W., and Southam, G. (2011). Microbially mediated mineral carbonation: roles of phototrophy and heterotrophy. *Environ. Sci. Technol.* 45, 9061–9068. doi: 10.1021/es201648g

Quast, C., Pruesse, E., Yilmaz, P., Gerken, J., Schweer, T., Yarza, P., et al. (2013). The SILVA ribosomal RNA gene database project: improved data processing and web-based tools. *Nucleic Acids Res.* 41, D590–D596. doi: 10.1093/nar/gks1219

Ripka, R., Deruelles, J., Waterbury, J. B., Herdman, M., and Stainer, R. Y. (1979). Generic assignment, strain histories and properties of pure cultures of cyanobacteria. *J. Gen. Microbiol.* 111, 1–61.

Rodriguez, . and Fraga, R. (1999). Phosphate solubilising bacteria and their role in plant growth promotion. *Biotech. Advances*, 17, 319–339.

Ruiz, F., Perlatti, F., Oliveira, D. P., and Ferreira, T. O. (2020). Revealing tropical technosols as an alternative for mine reclamation and waste management. *Fortschr. Mineral.* 10:110. doi: 10.3390/min10020110

Ryan, C. G., Siddons, D. P., Kirkham, R., Li, Z. Y., de Jonge, M. D., Paterson, D. J., et al. (2014). Maia X-ray fluorescence imaging: capturing detail in complex natural samples. *J. Phys. Conference Series.* 499:012002.

Sader, J., Leybourne, M., McClenaghan, M. B., and Hamilton, S. M. (2007). Low temperature serpentinization processes and kimberlite groundwater signatures in the Kirkland Lake and Lake Timiskiming kimberlite fields, Ontario, Canada: implications for diamond exploration. *Geochem. Explor. Environ. Anal.* 7, 3–21. doi: 10.1144/1467-7873/06-900

Sanna, A., Uibu, M., Caramanna, G., Kuusik, R., and Maroto-Valer, M. M. (2014). A review of mineral carbonation technologies to sequester CO_2. *Chem. Soc. Rev.* 43, 8049–8080. doi: 10.1039/C4CS00035H

Schloss, P. D., Westcott, S. L., Ryabin, T., Hall, J. R., Hartmann, M., Hollister, E. B., et al. (2009). Introducing mothur: open-source, platform-independent, community-supported software for describing and comparing microbial communities: Appl. *Environ. Microbiol.* 75, 7537–7541. doi: 10.1128/AEM.01541-09

Siddons, D.P., Kirkham, R., Ryan, C.G., De Geronimo, G., Dragone, A., Kuczewski, A.J., et al. (2014). Maia X-ray microprobe detector array system. In Journal of Physics: Conference Series 499:012001. IOP Publishing.

Sparks, R. S. J. (2013). Kimberlite Volcanism. *Annu. Rev. Earth Planet. Sci.* 41, 497–528. doi: 10.1146/annurev-earth-042711-105252

Uliasz-Bocheñczyk, A., and Mokrzycki, E. (2014). Mineral carbonation using natural materials: CO_2 reduction method. *Gospod. Surowc. Mineral.* 30, 99–110. doi: 10.2478/gospo-2014-0027

Wang, C., Harbottle, D., Liu, Q., and Xu, Z. (2014). Current state of fine mineral tailings treatment: a critical review on theory and practice. *Miner. Eng.* 58, 113–131. doi: 10.1016/j.mineng.2014.01.018

Wang, H. Y., Shen, L. I. U., Zhai, L. M., Zhang, J. Z., Ren, T. Z., Fan, B. Q., et al. (2015). Preparation and utilization of phosphate biofertilizers using agricultural waste. *J. Integr. Agric.* 14, 158–167. doi: 10.1016/S2095-3119(14)60760-7

Westcott, S. L., and Schloss, P. D. (2017). OptiClust, an improved method for assigning amplicon-based sequence data to operational taxonomic units. *mSphere* 2:2. doi: 10.1128/mSphereDirect.00073-17

Wickham, H., Averick, M., Bryan, J., Chang, W., McGowan, L. D. A., François, R., et al. (2019). Welcome to the Tidyverse. *J. Open Sour. Soft.* 4:1686. doi: 10.21105/joss.01686

Wilson, S. A., Dipple, G. M., Power, I. M., Barker, S. L. L., Fallon, S. J., and Southam, G. (2011). Subarctic weathering of mineral wastes provides a sink for atmospheric CO_2. *Environ. Sci. Technol.* 45, 7727–7736. doi: 10.1021/es202112y

Wilson, S. A., Dipple, G. M., Power, I. M., Thom, J. M., Anderson, R. G., Raudsepp, M., et al. (2009). Carbon dioxide fixation within mine wastes of ultramafic-hosted ore deposits: examples from the Clinton Creek and Cassiar chrysotile deposits. *Canada. Econ. Geol.* 104, 95–112. doi: 10.2113/gsecongeo.104.1.95

Xia, Y., Sun, J., Chen, D. G., Xia, Y., Sun, J., and Chen, D. G. (2018). Community diversity measures and calculations. *Statistical analysis of microbiome data with R.* ICSA Book Series in Statistics. 167–190.

Xiaofang, L., and Huang, L. (2014). Toward a new paradigm for tailings phytostabilization – nature of the substrates, amendment options and anthropogenic pedogenesis. *Criti. Rev. Environ. Sci. Technol.* 45, 813–839. doi: 10.1080/10643389.2014.921977

Xing, Q., Li, R., Zhang, X., Dong, X., Wang, D., and Zhang, L. (2015). Tailoring crystallization behavior of poly (L-lactide) with a low molecular weight aliphatic amide. *Coll. Poly. Sci.* 293, 3573–3583.

Yoda, I., Koseki, H., Tomita, M., Shida, T., Horiuchi, H., Sakoda, H., et al. (2014). Effect of surface roughness of biomaterials on Staphylococcus epidermidis adhesion. *BMC microbiology* 14, 1–7.